Analysis of the composite structures in diamond thin films by Raman spectroscopy

R. E. Shroder* and R. J. Nemanich
Department of Physics and Department of Materials Science and Engineering, North Carolina State University, Raleigh, North Carolina 27695-8202

J. T. Glass
Department of Materials Science and Engineering, North Carolina State University, Raleigh, North Carolina 27695-7907
(Received 15 August 1989)

Diamond and diamondlike thin films produced by various chemical-vapor-deposition processes have been examined using Raman spectroscopy. These films exhibit features in the Raman spectra, suggesting that they are composites of crystalline and amorphous diamond and graphitic structures. The components of this composite structure that contribute to the Raman scattering are discussed in terms of sp^2- and sp^3-bonded structures. The use of Raman spectroscopy as a technique for estimating the sp^2-to-sp^3 bonding ratio is considered. Powder composites of BN-diamond and graphite-diamond have been studied as a means of modeling the films, and a simple theoretical model of the Raman scattering from these samples is proposed. From these results it is shown that it is necessary to make assumptions about the domain size of the graphitic sp^2 regions. It is found that the Raman scattering associated with sp^2 bonding in the films is much stronger than that from single-crystalline or microcrystalline graphite structures. Shifts of the vibrational modes are also observed. The optical and vibrational properties of the sp^2 component in the films implies a different atomic microstructure. A model of the sp^2-bonding configurations in the films is proposed which may account for the observed features in the Raman spectra.

I. INTRODUCTION

Considerable attention has been focused recently on the growth of carbon films by plasma-enhanced chemical-vapor deposition (CVD) or similar methods.[1-8] The carbon films produced have generally been described as diamond[2,4,9] or diamondlike.[3,10,11] Some of these films have exhibited properties such as hardness, thermal conductivity, and optical band gaps which approach that of natural diamond. The films can be used as heat- and chemical-resistant optical coatings, and wear resistant mechanical coatings. Another application is for novel electronic devices. The mobilities of diamond are larger than those of Si, and the large band gap offers the possibility of high-temperature and/or high-power devices.

The CVD techniques use plasma or hot filaments or other methods to excite mixtures of methane or other hydrocarbon gases diluted in hydrogen. Typical gas ratios are 1% methane with a pressure of 30 torr. Substrate temperatures of 700–900 °C are often used. Variation in the process parameters leads to the formation of films with graphitic structures. Graphite is the stable crystalline form of carbon at ambient conditions, while diamond is metastable. The two crystalline forms exhibit different bonding often characterized as sp^3 for diamond and sp^2 for graphite. These two bonding configurations result in significantly different vibrational spectra, and Raman spectroscopy has proved particularly sensitive to the different structures.[12,13]

The question arises as to whether these various structures may coexist in CVD diamond and diamondlike films (i.e., the films are actually composites of the diamond and graphite structures discussed above). In a recent paper,[12] we explored these possibilities by examining the Raman spectra of diamond and diamondlike thin films. In this paper, we demonstrate the compositional nature of the films using Raman spectroscopy. The features of the different carbon structures are first identified. The features appearing in the Raman spectra of the films are compared to those of different carbon bonding structures, and the results are discussed in light of the composite structures present. We will also describe how the components of the composite can affect the corresponding Raman spectrum.

Several authors[14-16] have proposed methods to determine the sp^2-to-sp^3 bonding ratio in the films. The Raman technique may also be appropriate for making this determination. With this in mind, we have attempted to model the Raman scattering in the films by preparing composites of powders of boron nitride-diamond and graphite-diamond. The Raman results of the composites prepared from powders of BN and diamond and from graphite and diamond are presented, and a simple theoretical model of the Raman scattering is discussed. The Raman spectra from the diamond thin films also indicate that the optical absorption and Raman peak position of the sp^2-bonded structures is significantly different from that of natural graphite. We consider a model of these structures, similar to models proposed for a-C, in which the sp^2 bonding in the local microstructure is terminated in sp^3-bonded sites. This model may account for the observed features in the Raman spectra.

II. EXPERIMENT

The Raman-scattered light spectra were taken using the 5145-Å line of an Ar^+ laser. The diamond and diamondlike thin films were mounted in the backscattering configuration, and the scattered light was focused into a Spex model 1403 spectrometer equipped with a third monochromator and holographic gratings. A photomultiplier tube with photon-counting electronics was employed, and the entire system was controlled using an IBM PC/AT computer. The software used is unique in that it allowed for a single scan to be separated into several scanning regions.

In order to model the ratio of sp^2-to-sp^3 bonding in diamond thin films, composites of boron nitride-diamond and graphite-diamond powders were examined. These powders were obtained from commercially available sources.[17,18] Boron nitride was chosen because of its similar crystal structure to graphite, although, unlike graphite, it is optically transparent in the visible region so that effects on the Raman spectra due to absorption could be neglected. The diamond powder was slightly gray in appearance and of ~ 1 μm crystallite size. The graphite powder was black and very cohesive, and the boron nitride was white and also cohesive. Both materials contained crystallites of 30–40 μm size. Admittedly, this is large for our purposes, but we were primarily interested in the effects on the Raman spectra of the relative concentration of diamond in the composites. The examination of effects due to crystallite size was left for later.

The composites were created as follows; appropriate amounts of boron nitride and diamond powder were weighed, and the relative concentrations determined. We used wt. % (corrected for the atomic mass difference between BN and 2C) to describe the composites. In this way a 50% mixture would have the same number of B—N and C—C "molecules." The powders were then mixed using a mortar and pestle, and the resulting composites lightly pressed into aluminum sample holders. This process was then repeated for the graphite and diamond powders. These samples were also mounted in the backscattering configuration, and the Raman spectra were taken.

III. RESULTS AND DISCUSSION

A. Carbon film structures

The two common phases of carbon are graphite and diamond and both of these may be produced in the CVD process. Diamond is characterized by fourfold-coordinated sp^3 bonding of O_h symmetry.[19] Figure 1(a) shows the first-order Raman mode of natural diamond at 1332 cm^{-1}. This mode corresponds to a single triply-degenerate zone-center optical phonon, and is within 2 cm^{-1} of the highest-energy mode in the phonon dispersion curves of diamond. The threefold-coordinated sp^2-bonded structure of graphite may also be formed. The first-order Raman mode of graphite[20] at 1580 cm^{-1} is shown in Fig. 1(b). It is important to note that either crystalline or amorphous structures may be formed during deposition. By amorphous, we mean a network in which the local atomic bonding in the structure would be approximately tetrahedral for amorphous diamond, and planar threefold coordinated for amorphous graphitic structures. To our knowledge, the Raman spectra of amorphous diamond has not been reported, but assumptions can be made for its appearance by comparison to the spectrum of a-Si. In Fig. 1(a), we have scaled the Raman spectrum of a-Si to that of diamond using the ratio of the first-order Raman modes of the crystalline form of these two materials (520 cm^{-1}/1332 cm^{-1}). The Raman spectrum of amorphous graphite has been reported,[21] and the spectrum is overlayed on that of natural graphite in Fig. 1(b). Figure 1(c) shows the Raman spectrum of microcrystalline graphite. In this case the scattering at 1355 cm^{-1} is due to disorder-induced scattering from a strong peak in the vibrational density of states.[20] An important point of the comparison of these spectra is that sp^3 bonding yields Raman peaks at 1332 cm^{-1} or lower, while sp^2 bonding yields strong scattering with peaks ranging from 1355 to ~ 1600 cm^{-1}.

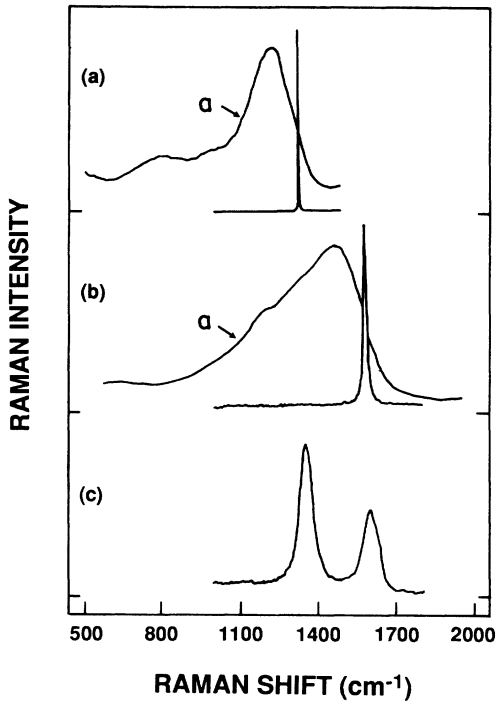

FIG. 1. Raman spectra of (a) diamond, (b) graphite, and (c) microcrystalline graphite. The solid lines in (a) and (b) represent the first-order spectra of crystalline diamond and graphite, respectively. The line in (a) labeled a is the spectrum of a-Si scaled to the diamond frequency to represent the spectrum of amorphous diamond, while the line in (b) labeled a is that due to amorphous graphite (from Ref. 21).

B. Diamond and diamondlike thin films

The Raman spectra of three carbon films produced under differing deposition conditions are shown in Fig. 2. Spectrum (a) shows features at 1355 and 1580 cm^{-1} which are similar to those associated with microcrystal-

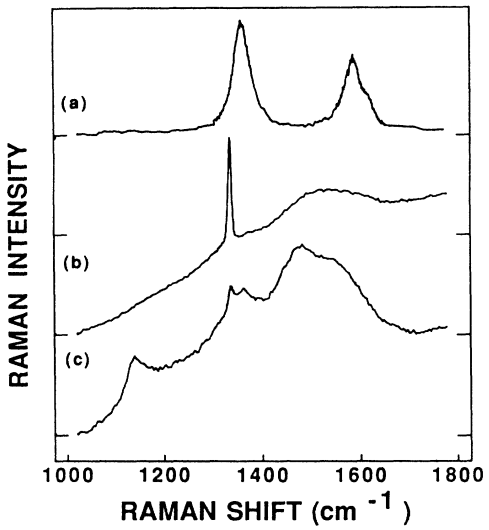

FIG. 2. First-order Raman spectra of diamond thin films. (a) Diamondlike film with features similar to microcrystalline graphite. (b) and (c) The sharp feature at 1322 cm^{-1} is indicative of crystalline diamond, while features between 1350 and 1600 cm^{-1} are attributed to sp^2-bonded carbon.

line graphite.[20] This type of film is generally described as "diamondlike" because of its physical properties such as semitransparency and hardness which are similar to diamond.[22] We have reported[12] the appearance of a peak in the second-order Raman spectrum of this material at $\sim$2940 cm^{-1} which is a combination of the two first-order modes given above. This peak indicates that both first-order modes are generated from the same region of the sample. Therefore, this type of film is predominated by sp^2-bonded microcrystalline graphitic structures, and is not considered a composite film. Regions of sp^3 bonding may exist in the film, but are not detected in the Raman scattering.

Spectrum (b) is dominated by the diamond peak at 1332 cm^{-1}, but also contains a broad feature at $\sim$1500 cm^{-1} which has been ascribed to regions of highly disordered graphite[2] or amorphous carbon.[22] As stated previously, the 1332-cm^{-1} mode of diamond is essentially the highest-energy vibrational mode of that structure; thus, none of the features in the Raman spectrum with energy higher than 1332 cm^{-1} can be attributed to diamond structures of long-range order. In comparison, spectrum (c) appears to be a linear combination of the features in (a) and (b). A peak at 1490 cm^{-1} is now the strongest feature in the spectrum, but the features of diamond and graphite structures are clearly seen. An additional feature is observed at 1140 cm^{-1} which is not observed in the other spectra. It has been proposed that this feature is due to disordered sp^3-bonded carbon which forms as a precursor to diamond formation.[12] Note that the peak at $\sim$1550 cm^{-1} is down-shifted from the position of the first-order mode of graphite (1580 cm^{-1}). This effect will be examined in more detail in Sec. III E. The two films described in (b) and (c) are often termed diamond films because of the presence of crystalline diamond. In this study, it is found that the size and absorption properties of these sp^2- and sp^3-bonded domains strongly affect the relative strengths of the Raman features described above. This will be discussed later in conjunction with the powder composition results. The details of Raman scattering from different carbon structures has been discussed elsewhere,[12] so a brief overview of Raman scattering from composites is presented.

C. Composite properties

In order to examine the Raman scattering from composites, three length scales are considered: micrometer scale, microcrystalline, and atomically disordered. (The term microcrystalline is used to represent submicrometer sizes typically less than 100 nm.) For micrometer-scale constituent materials, the Raman spectrum should appear as a linear combination of the features of the bulk materials. The absolute and relative intensities of the features will be strongly affected by the optical absorption of the two materials. These effects are clearly seen in the graphite-diamond composites where graphite is highly absorbing and diamond is effectively transparent in the visible range. Relative concentration and crystallite size are also very important to the resulting Raman spectrum. The details of these effects will be discussed later. As the domains decrease to microcrystalline scales, features should begin to appear in the Raman spectrum due to size effects associated with the breakdown of the conservation of wave vector.[20] Vibrational modes of the small crystallites are described as phonons with an uncertainty in the wave vector ($\Delta k \sim 2\pi/d$, where d is the domain size), and the momentum selection rules for the Raman process are, therefore, relaxed. The absorption depths and the phonon decay lengths for the constituent materials will generally be larger than the domain size. If the phonons are confined to the different regions, then the spectra will again be a superposition, but of microcrystalline components. Diffraction of the incident light will more uniformly illuminate the composite than would be the case for a micrometer-scale sample, and for very small domains optical absorption will not affect the relative intensities. If an atomically disordered composite were possible, the Raman spectrum would become the average of the vibrational and electronic properties of the disordered network. This spectrum would be quite different from the features of the bulk materials.

D. BN and diamond composites

Several of the Raman spectra taken from the BN and diamond composites are shown in Fig. 3. The two peaks exhibited are the first-order Raman mode of diamond at 1332 cm^{-1} and the first-order mode of BN which has been shown previously to occur at 1366 cm^{-1}.[23] The relative concentration of diamond in the samples ranges from $\sim$10% up to 66%. As is to be expected, the relative intensities of the two peaks change in proportion to the concentration of diamond present in the composite. If the ratio of the peak intensities of BN and diamond versus concentration of diamond in the samples is plotted, Fig. 4 is obtained. The data follow a smooth curve

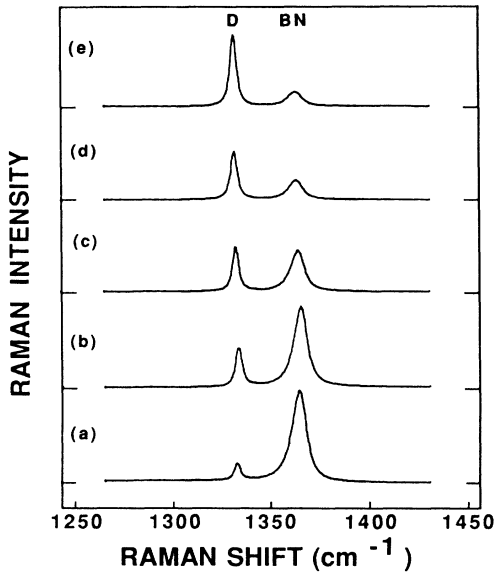

FIG. 3. First-order Raman spectra of the composites of diamond and BN powders. The relative concentrations of diamond in the samples are (a) 15%, (b) 20%, (c) 35%, (d) 55%, and (e) 67%. The features due to diamond (D) and BN are identified. The spectra have been multiplied by the indicated value.

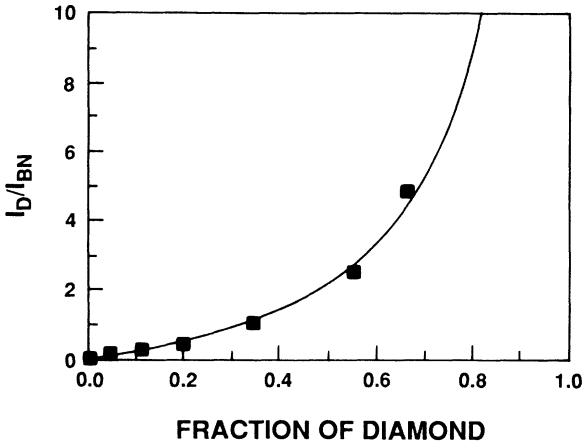

FIG. 4. Ratio of peak intensities (I_D/I_{BN}) vs relative concentration of diamond in the composite samples. Theoretical best fit assumes $a_{BN}/a_D \sim 2.9$.

which might be fitted very well using an appropriate model of the Raman scattering from composites.

In order to model the BN and diamond composites, we must understand the various parameters which effect the intensity of the Raman signal from these materials. Loudon[24] demonstrated that for a sample mounted in a backscattering geometry, the scattering intensity is given by

$$I = I_0 S/S + \alpha_1 + \alpha_2 \{1 - \exp[-(S + \alpha_1 + \alpha_2)L]\} , \quad (1)$$

where S is the scattering efficiency, I_0 is the incident intensity, L is the sample thickness in the direction of the incident laser light, and α_1 and α_2 are the absorption coefficients at the respective frequencies of the incident and scattered light. Wada and Solin[25] showed that this equation could be modified to give the ratio of the scattering intensities of two different materials:

$$\frac{I_D}{I} = \frac{I_{0D}}{I_0}\left[\frac{A_D}{A}\right]\left[\frac{L_D(\alpha_1+\alpha_2)}{1}\right]\left[\frac{\Delta\Omega_D}{\Delta\Omega}\right]\left[\frac{1-R_D}{1-R}\right]^2\left[\frac{\left[\sum_j (\hat{\mathbf{e}}_2\cdot\mathbf{R}_j\cdot\hat{\mathbf{e}}_1)^2\right]_D}{\left[\sum_j (\hat{\mathbf{e}}_2\cdot\mathbf{R}_j\cdot\hat{\mathbf{e}}_1)^2\right]}\right] , \quad (2)$$

where S has been redefined in terms of a scattering efficiency, A, and a summation over the inner product of the Raman tensor, $\mathbf{R}_j$, of the degenerate first-order mode and the polarization units vectors of the incident and scattered light, $\hat{\mathbf{e}}_1$ and $\hat{\mathbf{e}}_2$. I is the scattering intensity of the material being compared, and I_D represents the scattered intensity from the diamond power. I_0 is the incident intensity. $\Delta\Omega$ is the solid angle into which light is scattered, and the term in R corrects for reflection of the scattered light at the sample surface and multiple reflections in the sample as in diamond. Here, α_1 and α_2 are the previously defined absorption coefficients of the material to be compared to diamond since it has been assumed that diamond is transparent to the visibile laser radiation. The formulation assumes that $1/\alpha < L$ for the material to be compared to diamond.

If we now apply Eq. (2) to the composite samples, several approximations can be made. Since the Raman signal is being collected from a region of discrete particles, the values for L_D and $\Delta\Omega$ are the same for both materials. Also, our model will neglect the reflection losses due to light scattering between the BN and diamond particles. Finally, note that the last term in Eq. (2) provides unique values for the summations if the polarization directions of the incident and scattered light are known *a priori*. Since the BN and diamond composites contain particles of completely random orientation, an angle-averaged value of the summations over all possible polarization directions must be taken.

Using the above model, the ratio of the Raman-scattering intensities of diamond to BN may be written

$$\frac{I_D}{I_{BN}} \sim \frac{4A'_D N_D V_D}{3A'_{BN} N_{BN} V_{BN}} , \quad (3)$$

where A' is the angle- and polarization-averaged scatter-

ing efficiency per nearest-neighbor bond, N is the atomic density of BN or diamond, and V is the volume of material which is actually sampled by the Raman scattering. The factor of $\frac{4}{3}$ accounts for the fact that diamond contains four nearest neighbors and BN has three nearest neighbors at each site. In terms of P_D, the atomic percentage of diamond, $N_D V_D / N_{BN} V_{BN} = P_D/(1-P_D)$, so that Eq. (3) becomes

$$\frac{I_D}{I_{BN}} = \frac{4A'_D}{3A'_{BN}} \left[\frac{P_D}{1-P_D} \right] . \tag{4}$$

The first-order Raman mode in both diamond and BN is a bond-stretching mode. Using Eq. (4), we find excellent agreement with the data shown in Fig. 4 if the value for the ratio of the scattering efficiencies, A'_D/A'_{BN}, approximately equals 1.6. Using the fact that the ratio of the bond densities of diamond and BN is ~ 2, then $A_D/A_{BN} \sim 3.2$ (where A_D and A_{BN} are the scattering efficiencies per unit volume). This value is applicable to the BN and diamond powders, but not necessarily to the bulk materials.

E. Graphite and diamond composites

Since our model provides such good agreement with the data obtained from the BN and diamond particle composites, it might be modified to accurately predict the relative concentration of diamond in other types of composite samples. We have therefore extended this analysis to composites of graphite and diamond to determine if the same close agreement between theory and experiment might be found. Composite samples were prepared, and several of the Raman spectra obtained from these samples are shown in Fig. 5. The diamond peak at 1332 cm^{-1} is now accompanied by the first-order Raman mode of graphite[26] at 1580 cm^{-1}. The relative concentration of diamond in these samples ranges from $\sim 1\%$ up to 60%. It has been previously reported that the Raman efficiency of graphite is ~ 50 times larger than that of diamond.[25] An interesting aspect of these spectra is that the $\sim 1\%$ diamond composite displays a 1:1 ratio between the peak intensities of the first-order modes of diamond and graphite. At 50% diamond, it is seen that the peak due to graphite has practically disappeared. Thus the absorption of graphite has a significant effect on the Raman spectra of the composites, and is shown in the large disparity of the absolute intensity scales of the samples. This may be compared to the Raman spectra of the BN and diamond composites in Fig. 3 in which the absolute intensity scale is the same for all samples.

Again, the model described for the BN and diamond samples may be extended to the graphite and diamond composites if the effect of optical absorption due to graphite is included. Therefore, Eq. (3) can be written

$$\frac{I_D}{I_G} = \frac{4A'_D N_D V_D}{3A'_G N_G V'_G} = \frac{4A'_D N_D V_D}{3A'_G N_G V_G} \left[\frac{V_G}{V'_G} \right] , \tag{5}$$

where V'_G/V_G represents the *fraction* of each graphite particle sampled in the Raman process. Since the particle size is larger than the absorption depth of the graphite, this term accounts for only that portion of each graphite particle contributing to Eq. (5). Again, light incident on a diamond particle will sample the entire particle in the Raman process. Equation (5) can now be written in terms of P_D, the percentage of diamond in the composites:

$$\frac{I_D}{I_G} \sim \frac{4A'_D}{3A'_G} \left[\frac{P_D}{1-P_D} \right] \left[\frac{V_G}{V'_G} \right] . \tag{6}$$

From this analysis, it becomes apparent that the size and shape of the crystallites will affect the observed ratio of the Raman peaks. The geometric and absorption factors are accounted for in the V'_G/V_G term. At the 5145-Å exciting wavelength, graphite has an absorption depth[25] of ~ 300 Å. For simplicity, we have assumed that the graphite particles are cubic, and oriented with a flat surface toward the beam. Because the scattered light must also exit the absorbing region, the volume of graphite sampled will be a thin layer, ~ 150 Å thick, across the top of each graphite "cube."

It is important to note that the value for V'_G/V_G would increase for decreasing crystallite sizes, suggesting the graphite features would then appear more strongly in the Raman spectrum of very-fine-grain particles. The results of this model are demonstrated in Fig. 6, where the ratio of the two peaks versus concentration of diamond is again plotted along with several fitting curves based on Eq. (6). For these calculations we have determined A'_D/A'_G as follows. The ratio of the scattering efficiencies per unit volume was reported by Wada and Solin to be $\sim 1/50$.[26] They noted a significant uncertainty depending on which values of the optical constants were used.[25] In our model we have considered the scattering in terms of the number of nearest-neighbor C—C bonds. The ratio of the bond density of graphite to

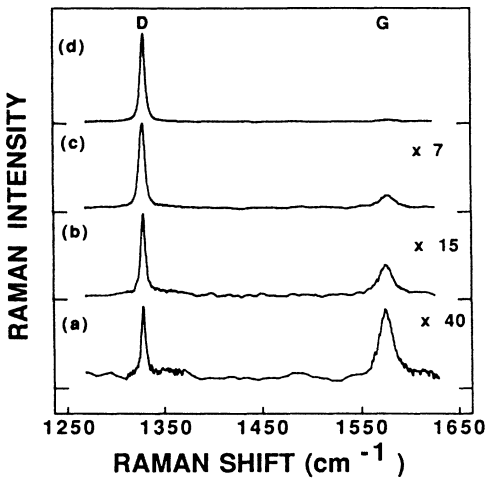

FIG. 5. First-order Raman spectra of the composites of diamond and graphite powders. The relative concentrations of diamond in the samples are (a) 1.3%, (b) 6.6%, (c) 21.5%, and (d) 50.0%. The features due to diamond (D) and graphite (G) are identified. The spectra have been multiplied by the indicated value.

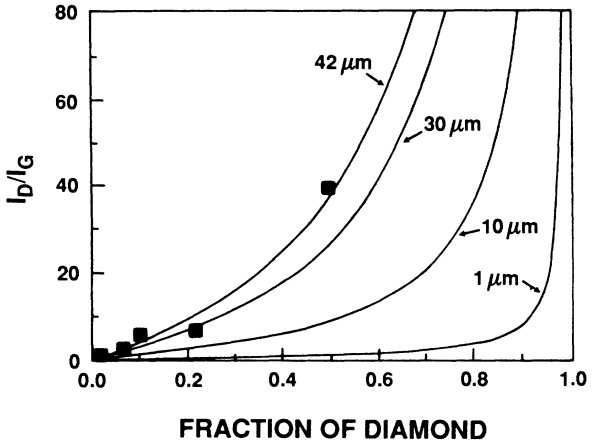

FIG. 6. Ratio of peak intensities (I_D/I_G) vs relative concentration of diamond in the composite samples. The solid lines are derived from Eq. (6) assuming an average graphite particle size of 30, 10, and 1 μm, respectively.

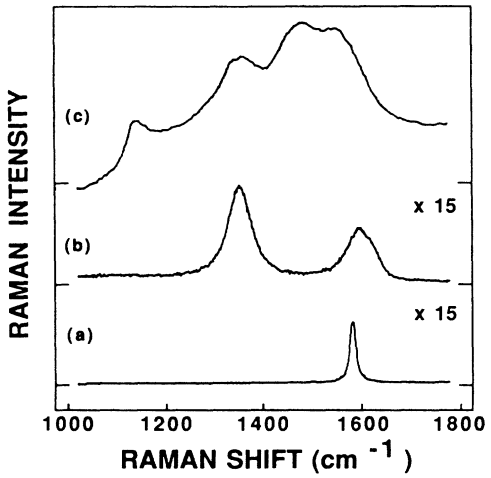

FIG. 7. First-order Raman spectra of (a) highly oriented pyrolytic graphite, (b) glassy carbon, and (c) diamond thin film produced by microwave-plasma-excited CVD. The spectra have been multiplied by the indicated value.

diamond is 0.48. Thus the value of A_D'/A_G' will be $\sim 1/100$ in terms of scattering per nearest-neighbor bond. Theoretical curves are shown assuming "cubic" graphite particles of 42, 30, 10, and 1 μm size. The model, using 42-μm "cubes," follows the data very well. The curves for 10 and 1 μm particle size indicate that the diamond peak would begin to dominate the spectrum only at high concentrations of diamond. Clearly the observed ratio is strongly dependent on the crystallite size.

The model reaches a limit where the crystalline domains are smaller than the absorption length of the absorption regions. In this limit, the value of V_G'/V_G becomes 1 and the effects of absorption can be ignored. The relation is then the same as that for two transparent materials as in Eq. (4).

F. Graphitic bonding in diamond films

While the Raman spectra of the CVD carbon films show diamond crystal structures, they also display features indicating sp^2 bonding in the films. The Raman spectra of one of the films are compared to highly oriented pyrolytic graphite (HOPG) and microcrystalline or "glassy" carbon in Fig. 7. The features in the film are broader than those of the graphitic compound, but they clearly represent the presence of sp^2 bonding. Spectrum (a) of HOPG and (b) of glassy carbon display the 1580-cm^{-1} peak characteristic of crystalline or microcrystalline graphite. We also note again that the highest-frequency peak in the film is down-shifted from that of the graphitic materials. The absolute intensity scales of the graphitic materials are approximately equal. By comparison, the Raman spectrum of the composite diamond thin film in Fig. 7(c) shows an absolute intensity scale ~ 15 times greater than that of HOPG or glassy carbon. This implies that the features in spectrum (c) at 1355 and 1580 cm^{-1} must be associated with structures having optical properties quite different from those of graphite.

The two parameters related to the bonding structure which can affect the absolute Raman intensity are the scattering cross section, A, and the absorption coefficients, α_1 and α_2. Since the Raman cross section for diamond is less than that for graphite, we would suggest that microstructural changes would not tend to increase the Raman cross section of the sp^2 regions. Let us, therefore, consider the optical absorption. At an sp^2 site, three of the four valence electrons form in-plane σ bonds, while the fourth enters a π orbital lying perpendicular to this plane. Note that in graphite the π orbitals are not localized at their respective sp^2 sites, but can move relatively freely among the C atoms. This does not lead to true C=C "double" bonds, but nevertheless the π bonds contribute to the bond strength of the in-plane bonds. Since they are weakly bonding, the π states lie closest to the Fermi level, E_F. Therefore, π-π^* transitions occur at lower energies than σ-σ^* transitions and account for the strong optical absorption in graphite. Savvides[14] has considered the optical properties associated with a-C containing no hydrogen. He demonstrated that in a matrix of sp^2 and sp^3 sites the density of states at the top of the valence band decreases as the relative concentration of sp^3 sites increases. Therefore, incorporation of sp^3 sites into the network leads to an increasing optical gap and, consequently, lower optical absorption. More recently, Robertson and O'Reilly[27] have followed the model of a-C suggested by Wada *et al.*,[22] and proposed that an a-C network should consist of ~ 15-Å graphitic "islands" of fused sixfold rings surrounded by sp^3 sites. The π bonds would be broken at the island boundary as a mechanism for relieving strain in the network. This model also suggests a higher optical gap with decreasing absorption.

The incorporation of very small graphitic regions in the diamond films could then lead to a lowering of the optical absorption of the regions and an enhanced Raman intensity. In this limit, the nearby diamond and graphitic regions would be uniformly illuminated, and our analysis would suggest that the Raman scattering from sp^2-bonded materials should be ~ 100 times stronger than

that from diamond regions.

We have analyzed the integrated Raman intensities of the spectra shown in Figs. 2(b) and 2(c). If the integrated Raman intensities of the sp^2 and diamond peaks are used, and the 100-fold difference in scattering efficiencies, we obtain 87% and 28% diamond, respectively. Transmission-electron-microscopy (TEM) measurements of films similar to that used to obtain the spectrum shown in Fig. 2(c) show predominantly diamond structures.[8] Therefore, the number of sp^2 regions is still higher than would be anticipated from TEM. One possibility of accounting for this enhancement is that the microcrystalline regions lead to disorder-induced scattering from the breakdown in the wave-vector selection rules for the Raman scattering,[23] and this adds an additional correction.

In addition to the apparent optical properties of the sp^2 component in the diamond films, we also observed that the highest-energy feature in the Raman spectra of the films occurs at ~ 1550 cm^{-1}, and this is down-shifted from the expected position of graphite at ~ 1580 cm^{-1}. We considered whether this might be due to the convolution of the 1580-cm^{-1} peak with the feature due to amorphous sp^2 structures at ~ 1480 cm^{-1}. In order to examine this, we formed a computer-generated linear combination of the Raman spectra of a diamond thin film and a sample of microcrystalline graphite, similar to Figs. 2(a) and 2(c). The various peaks were scaled to approximately the same absolute intensity as the features in Fig. 2(b). This "combined" spectrum is shown in Fig. 8(a), and is compared to other similar spectra from various diamond thin films. Figures 8(b) and 8(c) were taken from films created by a microwave-plasma-excited CVC process in which the CH_4/H_2 dilution was 1.5% and 3.0%, respectively. The spectrum in Fig. 8(d) was obtained from a "just-nucleated" diamond sample in which the surface coverage was $\sim 50\%$. All three samples show approximately the same Raman features. The spectra clearly demonstrate, when compared to Fig. 8(a), that the peak at ~ 1550 cm^{-1} must be down-shifted from ~ 1580 cm^{-1}, and is not due to a convolution of peaks.

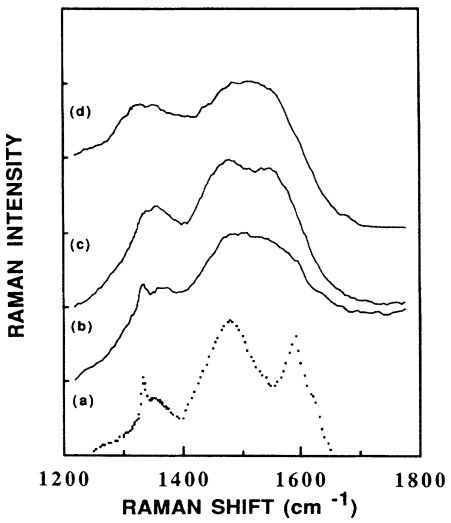

FIG. 8. Comparison of Raman spectra from CVD diamond films and computer model to examine down shift of highest-energy peak. (a) Computer-generated Raman spectra assuming linear combination of spectra of diamond thin film and microcrystalline graphite (b) deposited at 1.5% CH_4/H_2 concentration, (c) deposited at 3.0% CH_4/H_2 concentration, and (d) "just-nucleated" diamond film with substrate coverage $\sim 50\%$.

Several authors[22,28,29] have noted similar down shifts in the Raman spectra of a-C:H. All of these films contained >30 at. % H though, whereas the films examined in this paper were deposited at temperatures $>800\,^{\circ}$C such that they contained <1 at. % H. Ramsteiner and Wagner[28] also showed that upon annealing their a-C:H films to 600 °C almost all H was removed from the samples, leaving sp^2-bonded microcrystalline graphite, and the first-order mode was observed at the unshifted ~ 1580-cm^{-1} frequency. Dillon *et al.*[30] have used Raman spectroscopy to examine a-C films produced by ion-beam sputtering and by rf-plasma deposition. The ion-beam-sputtered samples, containing little H, also showed a down shift in the first-order mode, but the disorder mode at 1355 cm^{-1} was not distinct from the background. Upon annealing to 400 °C, the disorder mode became apparent at ~ 1355 cm^{-1}, and the first-order mode was slightly down-shifted. Higher-temperature annealing restored this feature to its original value. Their analysis focused on the continuous-random-network models of Beeman[31] which assumed bond-angle distortion and the existence of fourfold coordination in the films to explain the Raman features.

We can now consider both the optical and vibrational properties of the sp^2 component in diamond thin films, in order to provide a clearer picture of the nature of the bonding. The vibrational properties show two sp^2 components, one similar to amorphous carbon and one that is graphitic. The peak intensity at 1355 cm^{-1} indicates that the microcrystalline domain sizes are less than 30 Å.[26] In the light of the disparity in the Raman intensity, the model proposed by Robertson and O'Reilly[27] seems to be valid for diamond thin films; namely the sp^2 graphitic regions are small and are terminated at sp^3 sites, resulting in lower optical absorption. This possibility is also consistent with TEM measurements which show that the graphitic regions apparently lie between regions of crystalline or microcrystalline diamond. The decreased density of π states at the top of the valence band would lower the absorption, and their localization at an sp^3 site would decrease the corresponding bond strength. The weaker bonding can then account for the down shift in the first-order Raman mode of the graphitic regions. The graphitic regions do not have to be limited to 15–20-Å island structures, but it seems unlikely that much larger structures would produce the same results. This is because larger structures would have a smaller percentage of sites terminated in sp^3 bonding; thus, the optical properties would be more heavily influenced by the bulk structure. Disordered regions must also be assumed to explain the appearance of the feature at ~ 1480 cm^{-1}, but how this disorder is incorporated into the polycrystalline film is uncertain.

IV. CONCLUDING REMARKS

The Raman spectra of various diamond and diamondlike thin films have been examined. The features displayed by the diamond films suggest that they are composities of sp^2 and sp^3 bonding. We have attempted to understand the nature of these films using composites of BN-diamond and graphite—diamond powder samples. A simple model of the Raman scattering from these composites has been proposed, and reasonable agreement with the experimental data has been obtained. This investigation of graphite and diamond composites demonstrates that both concentration and crystallite size have significant effects on the resulting Raman spectra. In diamond films containing regions of diamond and graphite, it is predicted that the Raman spectra could be used to estimate the relative concentrations of these regions, but we emphasize that the sizes of the various domains in the films must first be known. We have found that the characteristics of the sp^2 bonding in the films do not correlate well to regions of microcrystalline graphite. The Raman spectra suggest that the optical absorption of these regions in the visible is less than in natural graphite for the wavelength used. Also, a peak exhibited in the Raman spectra at 1550 cm^{-1} is down-shifted from the position of the first-order Raman mode of graphite, but a peak at 1355 cm^{-1}, corresponding to a disorder mode in small graphite crystallites, is still observed. We have proposed a model in which the π bonds in the graphitic regions are localized or attached to sp^3 sites. This model can account for the features observed in the Raman spectra of the diamond thin films.

ACKNOWLEDGMENTS

We gratefully acknowledge K. Kobashi and Y. Kawate of Kobe Steel, Ltd., for supplying the diamond samples used in this study. We also appreciate the helpful discussions of R. Rudder of the Research Triangle Institute and B. Williams of North Carolina State University (NCSU), as well as the help of R. Russell of NCSU in the preparation of the composite powder samples, and Shannon Wells of NCSU for data analysis. This work was supported in part by SDIO/IST through the U.S. Office of Naval Research under Contract No. N00014-86-K-0666.

---

*Present address: Rocketdyne Div., Rockwell Int., Canoga Park, CA 91303.

[1]B. V. Derjaguin, B. V. Spitsyn, A. E. Gorodetsky, A. P. Zacharov, L. I. Bouilov, and A. E. Aleksenko, J. Cryst. Growth **31**, 44 (1975).

[2]S. Matsumoto, Y. Sato, M. Tsutsumi, and N. Setaka, J. Mater. Sci. **17**, 3106 (1982).

[3]T. Mori and Y. Namba, J. Appl. Phys. **55**, 3276 (1984).

[4]A. Sawabe and T. Inuzuka, Thin Solid Films **137**, 89 (1986).

[5]C. P. Chang, D. L. Flamm, D. E. Ibbotson, and J. A. Mucha, J. Appl. Phys. **63**, 1744 (1988).

[6]B. Singh, O. R. Mesker, A. W. Levine, and Y. Arie, Appl. Phys. Lett. **52**, 1658 (1988).

[7]K. Ito, T. Ito, and I. Hosoya, Chem. Lett. **1988**, 589.

[8]B. E. Williams and J. T. Glass, J. Mater. Res. **4**, 373 (1989).

[9]Y. Hirose and Y. Terawasa, Jpn. J. Appl. Phys. **25**, L519 (1986).

[10]C. B. Zarowin, N. Venkataramanan, and R. R. Poole, Appl. Phys. Lett. **48**, 759 (1986).

[11]V. Natarajan, J. D. Lamb, J. A. Woollam, D. C. Liu, and D. A. Gulino, J. Vac. Sci. Technol. A **3**, 681 (1985).

[12]R. J. Nemanich, J. T. Glass, G. Lucovsky, and R. E. Shroder, J. Vac. Sci. Technol. A **6**, 1783 (1988).

[13]D. S. Knight and W. B. White, J. Mater. Res. **4**, 385 (1989).

[14]N. Savvides, J. Appl. Phys. **58**, 518 (1985).

[15]S. Kaplan, F. Jansen, and M. Machonkin, Appl. Phys. Lett. **47**, 750 (1985).

[16]S. D. Berger, D. R. McKenzie, and P. J. Martin, Philos. Mag. Lett. **57**, 285 (1988).

[17]The BN and diamond powders were obtained from AESAR Chemical, Seabrook, NH 03874.

[18]The graphite powder was obtained from ALFA Chemical, Danvers, MD, 01923.

[19]S. A. Solin and A. K. Ramdas, Phys. Rev. B **1**, 1687 (1970).

[20]R. J. Nemanich and S. A. Solin, Phys. Rev. B **20**, 392 (1979).

[21]S. A. Solin and R. J. Kobliska, in *Amorphous and Liquid Semiconductors*, edited by J. Stuke (Taylor and Francis, London, 1974), p. 1251.

[22]N. Wada, P. J. Gaczi, and S. A. Solin J. Non-Cryst. Solids **35&36**, 543 (1980).

[23]R. J. Nemanich, S. A. Solin, and R. M. Martin, Phys. Rev. B **23**, 6348 (1981).

[24]R. Loudon, J. Phys. **26**, 677 (1964).

[25]N. Wada and S. A. Solin, Physica B+C **105B**, 353 (1981).

[26]F. Tuinsta and J. L. Koenig, J. Chem. Phys. **53**, 1126 (1970).

[27]J. Robertson and E. P. O'Reilly, Phys. Rev. B **35**, 2946 (1987).

[28]M. Ramsteiner and J. Wagner, Appl. Phys. Lett. **51**, 1355 (1987).

[29]M. Yoshikawa, G. Katagiri, H. Ishida, A. Ishitani, and T. Akamatsu, Appl. Phys. Lett. **52**, 1639 (1988).

[30]R. O. Dillon, J. A. Woollam, and V. Katkanant, Phys. Rev. B **29**, 3482 (1984).

[31]D. Beeman, J. Silverman, R. Lynds, and M. R. Anderson, Phys. Rev. B **30**, 870 (1984).